# UNSUPERVISED LEARNING FOR TEMPORAL SEARCH SPACE REDUCTION IN THREE-DIMENSIONAL SCENE RECOVERY

Tom Warsop and Sameer Singh
*Research School of Informatics, Holywell Park, Loughborough University, Leicestershire, LE11 3TU, U.K.*

Keywords: Three-dimensional scene recovery, Search space reduction, Unsupervised learning.

Abstract: Methods for three-dimensional scene recovery traverse scene spaces (typically along epipolar lines) to compute two-dimensional image feature correspondences. These methods ignore potentially useful temporal information presented by previously processed frames, which can be used to decrease search space traversal. In this work, we present a general framework which models relationships between image information and recovered scene information specifically for the purpose of improving efficiency of three-dimensional scene recovery. We further present three different methods implementing this framework using either a naive Nearest Neighbour approach or a more sophisticated collection of associated Gaussians. Whilst all three methods provide a decrease in search space traversal, it is the Gaussian-based method which performs best, as the other methods are subject to the (demonstrated) unwanted behaviours of convergence and oscillation.

## 1 INTRODUCTION

Recovering three-dimensional (3D) scene information from two-dimensional (2D) image information can be very useful. The work presented in this paper is part of a larger project concerned with recovering 3D scene information from a train mounted, forward-facing camera.

Many methods have previously been applied to 3D scene recovery. As highlighted by (Favaro et al., 2003), a large proportion of these methods follow a similar pattern of execution. First point-to-point correspondences among different images are established. These image correspondences are then used to infer three-dimensional geometry. These feature correspondences can be computed in one of two ways, either by seaching the 2D image plane or by incorporating epipolar geometry.

The first set of methods do not take the 3D nature of the problem into account. These methods typically operate in two steps. First, image features are detected. Methods presented in literature use Harris corners ((Li et al., 2006)), SIFT features ((Zhang et al., 2010)) and SURF features ((Bay et al., 2008)). More recently, to compensate for viewpoint changes in captured image information (Chekhlov and Mayol-Cuevas, 2008) artifically enhanced the feature set for a single image point considered, computing spatial gradient descriptors for multiple affine transformed versions of the image area surrounding a feature point. Feature correspondences are then computed by feature matching in subsequent frames.

It is, however, possible to incorporate 3D information into these feature correspondence computations. One of the most straightforward ways of integrating 3D information uses stereo cameras. Under schemes such as these, as can be seen in the work of (Zhang et al., 2009; Fabbri and Kimia, 2010; Li et al., 2010) and (Grinberg et al., 2010) (to name a few) epipolar scanlines across left and right-hand images are searched for matching feature correspondence. It is possible to integrate these concepts into monocular camera configurations such as in the method introduced by (Klein and Murray, 2007) known as *Parallel Tracking and Mapping (PTAM)*. In which features are initialised with their 3D positions by searching along epipolar lines, defined by depth between key frames of the image sequence. (Davison, 2003; Davison et al., 2007) presented a similar idea of feature initialisation in *monoSLAM*.

When recovering 3D information from image sequences, if they are processed in reverse chronological order *new* scene elements to process appear at image edges. This provides an interesting property - image areas recovered in subsequent image frames exhibit similar properties to those processed previously, highlighted in Figure 1. It may therefore be possible to exploit this information, using relationships be-

Warsop T. and Singh S..
UNSUPERVISED LEARNING FOR TEMPORAL SEARCH SPACE REDUCTION IN THREE-DIMENSIONAL SCENE RECOVERY.
DOI: 10.5220/0003308405490554
In *Proceedings of the International Conference on Computer Vision Theory and Applications* (VISAPP-2011), pages 549-554
ISBN: 978-989-8425-47-8

tween 2D image features and recovered 3D scenes to reduce the size of the search spaces traversed (for example, along epipolar lines) when computing feature correspondences. Such a concept has not been proposed by previous methods and forms the basis of the method presented in this work (named Temporal Search space Reduction, or TSR).


Figure 1: When processing image sequences in reverse order, *new* scene elements entering at image edges exhibit similar 2D image and 3D scene properties.

The structure of the remainder of this paper is as follows. Section 2 presents a brief overview of the 3D scene recovery method used as a platform for experimental comparison of the TSR extension. The TSR concept and three implementations are discussed in section 3. Experimental results regarding real data are provided in section 4, as is the discussion of problems faced by methods implementing the TSR concept. Finally, section 5 concludes the work in this paper.

## 2 THREE-DIMENSIONAL SEQUENCE RECOVERY

To demonstrate the TSR concept, the 3D scene recovery method described by (Warsop and Singh, 2010) is used. This method has been chosen because it can be simply adapted to recover dense 3D scene information in the form of planes, in which correspondences are searched for along categorized epipolar lines. This method recovers the 3D corner points of a plane related to image quadrilaterals by searching for the 3D corner values which provide the lowest reprojection error in a subsequent frame. Summarized as:

$$P_{3D} = min_{Q_{3D}}\{SAD(S_1, SQR(R(Q_{3D}, I_2), I_2))\} \quad (1)$$

where, $SAD(x,y)$ computes the sum-of-absolute differences in the RGB channels of images $x$ and $y$, $R(Q,I)$ reprojects the 3D coordinates of $Q$ into subsequent image $I$, $SQR(q,I)$ converts a quadrilteral image area $q$ into a square area using image data $I$, $S_1 = SQR(Q_1, I_1)$ where $Q_1$ and $I_1$ are the original quadrilateral and image under consideration (respectively) and $Q_{3D}$ are the 3D coordinates of the quadrilateral corner points searched through. The adaptation

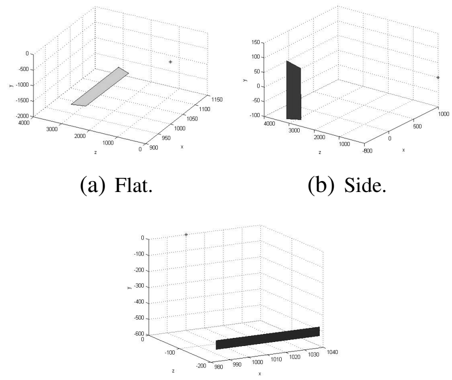

(a) Flat. (b) Side.

(c) Vertical.

Figure 2: The three base types of plane used for searching in the 3D scene recovery method.

made to this method takes the form of only using three types of planes (shown in Figure 2) when searching for the best matching plane - defined by height, width and depth respectively.



## 3 UNSUPERVISED LEARNING FOR TEMPORAL SEARCH SPACE REDUCTION

Figure 3 demonstrates how the concept proposed by TSR (shaded boxes) integrates with a typical 3D scene recovery method (unshaded boxes). The following describes each shaded box:

1. **Compute 2D Image Features** - since the image area surrounding a feature is to be used to indicate the 3D search space to traverse, these features must be computed.

2. **(2D,3D) Relationship Model** - storing the relationship between 2D image features and corresponding recovered 3D information.

3. **Compute 3D Search Space** - for any new feature considered for recovery, the range of 3D values to consider should be selected based upon the computed 2D values. If similar features have been processed before, narrow ranges around expected values should be searched. Otherwise, large ranges should be selected. These search ranges are defined by a category type (flat, vertical or side) and value (height, depth or width).

4. **Update the Model** - once a new feaure has been recovered, the model storing the 2D and 3D relationships must be updated to include this new information.

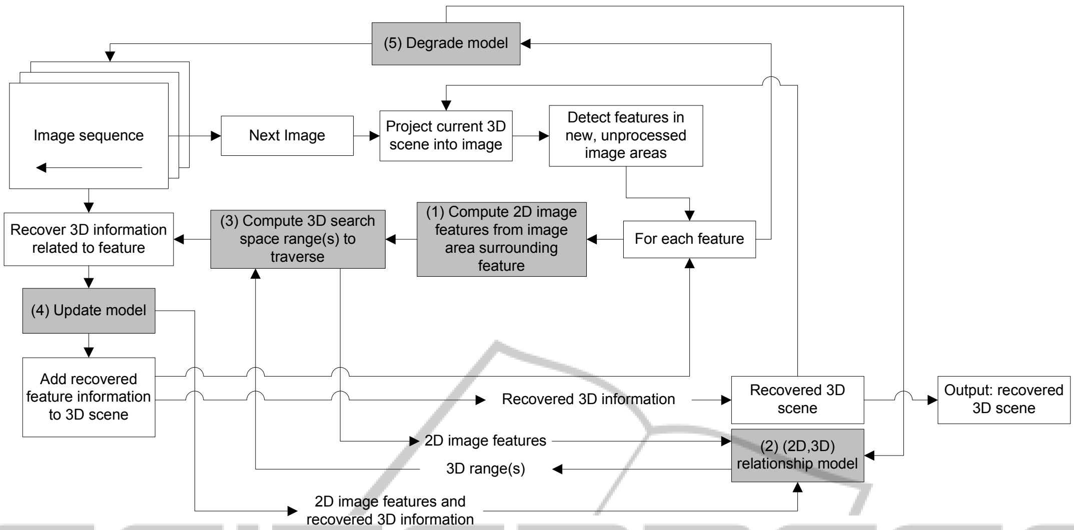


Figure 3: 3D sequence recovery method (unshaded box) enhancement, incorporating temporal information stored as a relationship between 2D image information of the area surrounding a feature and corresponding recovered 3D information. The grey shaded boxes represent the additions proposed by TSR.



**5. Model Degradation** - it is necessary to degrade the model on each iteration, preventing it from consuming too much memory.

The following subsections discuss three different methods for implementing these proposed TSR extensions. Each method uses the same image features - for each image quadrilateral area considered separate red, green and blue histograms are computed. From which each of the mean, standard deviation, skewness, kurtosis and energy are computed, resulting in 15 features.

## 3.1 Nearest Neighbour (NN)

The first implementation stores the (2D,3D) relationship as a list of tuples ($M$) of the form: $<$ 2D image features, category, value $>$. For any newly processed quadrilateral, the categories to process are determined by computing the following value for each category, $c \in$ flat, side, vertical:

$$p_c = \frac{1}{\sqrt{2\pi\sigma_{Nc}^2}} e^{\frac{-(f-\mu_{Nc})^2}{2\sigma_{Nc}^2}} \quad (2)$$

where, $f$ are the 2D image features of the currently considered quadrilateral, $Nc$ represents the $K$ Euclidean nearest neighbours to $f$ in $M$ of category $c$, $\mu_{Nc}$ and $\sigma_{Nc}$ are the mean and standard deviation of $Nc$ respectively. The resultant set of probabilities are normalized and any above a threshold indicate the corresponding categories should be processed. The range of values to process for any chosen category are defined by a minimum and maximum value computed using:

$$min_c = \mu_v - (D\sigma_v \times (1 - p_c)) \quad (3)$$

$$max_c = \mu_v + (D\sigma_v \times (1 - p_c)) \quad (4)$$

where, $\mu_v$ and $\sigma_v$ are the mean and standard deviation of the 3D values associated with $Nc$ and $D$ is a scalar value. Scene recovery results are used to create new tuples to update $M$ with. To implement model degradation, an extra *distance* field is used in the tuples of $M$. When a tuple is added to $M$, this field is initialised to zero and accumulates the distance travelled by the camera since initialisation. A threshold of this distance field can then be used to remove *old* tuples.

## 3.2 Nearest Neighbour with Error Correction (NNEC)

The second implementation proceeds as the previous NN method. But with the addition that after recovery has been performed the SAD value associated with the best set of quadrilateral corners ($BQ_{3D}$) is computed:

$$min_{SAD} = SAD(S_1, SQR(R(BQ_{3D}, I_2), I_2)) \quad (5)$$

where everything has the same meaning as in Equation 1. If $min_{SAD}$ is greater than a pre-determined threshold, the value ranges selected for processing by the nearest neighbour metric are deemed to of been inappropriate and recovery is performed again, using all value ranges. The subsequent result is added to the tuple list as before.

### 3.3 Feature and Value Gaussians (FVG)

The relationship model of this implementation builds a set of Gaussian distributions for the 2D image features encountered. Similar 2D image features are represented by a single multi-dimensional Gaussian distribution. Each of these *feature* distributions is associated with value range distributions, each representing similar 3D values that have been recovered for the corresponding 2D image features. Each value distribution also has an associated category.

For any new feaure recovered, the probability the corresponding image features ($f$) belong to any of the feature distributions are computed:

$$p_{FD} = \frac{1}{\sqrt{2\pi\sigma_{FD}^2}} e^{\frac{-(f-\mu_{FD})^2}{2\sigma_{FD}^2}} \tag{6}$$

where, $p_{FD}$ is computed for each of the feature distributions, $FD$ is the current feature distribution under consideration and $\mu_{FD}$ ad $\sigma_{FD}$ are the mean and standard deviation of $FD$ respectively. For each $p_{FD}$ greater than a pre-determined threshold, the associated value distributions are each considered in turn and used to determine a value range to process, using the minimum and maximum computed in a similar manner to Equations 3 and 4. If $VR$ represents the set of all values to process of a new feature, the best fitting plane for the considered 3D scene recovery method is computed using:

$$P_{3D} = min_{Q_{3D} \in VR}\{SAD(S_1, SQR(R(Q_{3D}, I_2), I_2))\} \tag{7}$$

If the SAD value associated with $P_{3D}$ is greater than a threshold, reprocessing proceeds as for the NNEC method. Under this scheme, there are three possible ways in which the model can be updated. These are demonstrated in Figure 4, where green represents update and red means a new distribution is added. Model degradation is performed by storing a *distance since last update* with each distribution, where distance is in terms of camera movement. If this distance exceeds a threshold the corresponding Gaussian is removed.

# 4 EXPERIMENTAL RESULTS

The data used for experimentation consists of high-definition (i.e. 1920 × 1080 pixels) image frames, captured from a front-forward facing camera mounted on a train. In total, 5 sequences totalling 520 image frames were used. Each image frame was ground truthed by hand - matching approximately 850 features between image pairs.

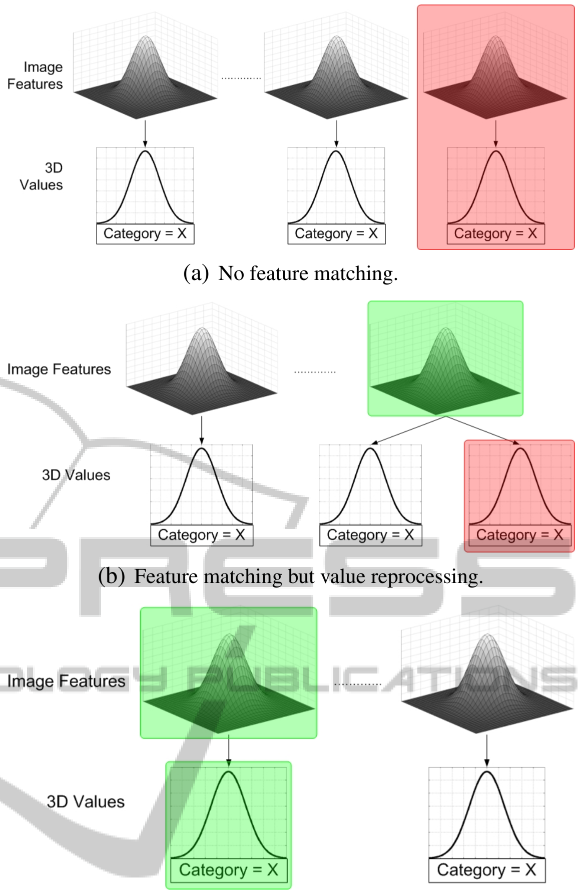


(a) No feature matching.

(b) Feature matching but value reprocessing.

(c) Feature matching and no value reprocessing.

Figure 4: Graphical repesentation of the three different types of update in FVG.

With regards to TSR methods presented in section 3, Figure 5(a) presents the average number of combinations checked per quadrilateral recovered in each frame and Figure 5(b) the accuracy of each method, where *Exhaustive* refers to the unaltered method described in section 2. The results show that each of the methods implementing the TSR extensions provides a decrease in the number of combinations checked per recovered quadrilateral whilst maintaining similar accuracy. However, this reduction sometimes comes at a cost. For example, the NN method produces less accurate scene recovery results. This is because the NN relationship model can converge. Consider a synthetic image sequence comprising of only a textured wall and floor plane such as in Figure 6. The sequence was created such that in the first 10 images, the wall is of a fixed $x$-coordinate of 400. Then in the 19th image the wall was created with an $x$-coordinate of 0.

In the first 18 images of the sequence, the whole image was processed and used to update the NN model. In the 19th image only a square of the wall

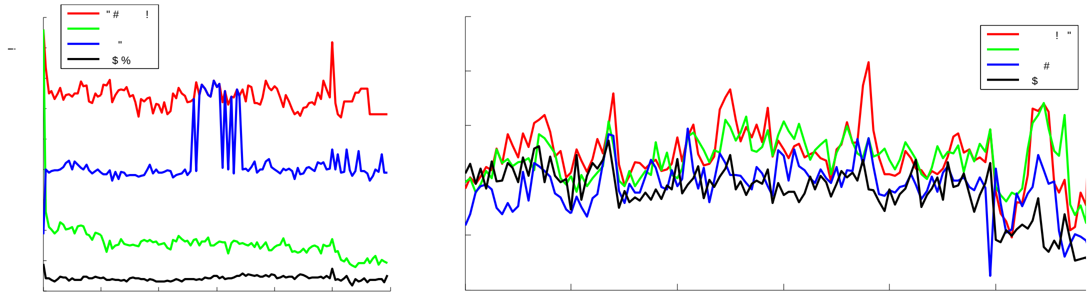

(a) Average number of quadrilterals checked per sequence frame.

(b) Average difference between recovered sequence frames and ground truth.

Figure 5: Comparison of the number of checks made and difference with ground truthed scene per method, averaged over all 5 sequences.

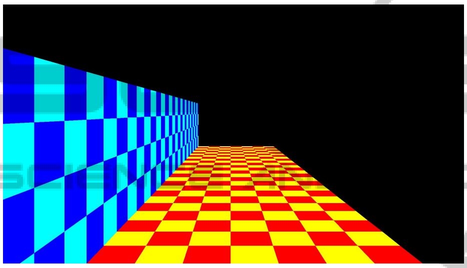

Figure 6: Synthetic image sequence example comprising of a floor and wall plane.

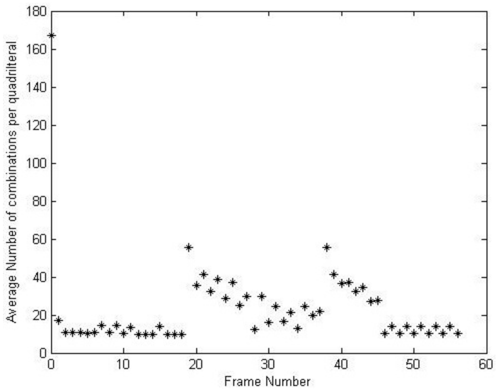


Figure 7: Number of combinaions procesed by the NNEC method for the oscillating wall sequence.

plane was recovered. As expected, the *side* plane category was chosen. However, because all previous *side* planes processed are of width 400, the value range chosen to process is 390.50 to 421.04. Clearly this is incorrect. The error occurs because for a large part of the sequence one set of 2D image features maps to one specific 3D value. Hence, the model converges for these 2D image features. When the 3D value changes for this specific set of features the model cannot represent this, resulting in possible error.

NNEC resolves this convergence issue. However because of the nearest neighbour selection scheme, this method can produce oscillatory behaviour. For example, consider a similar synthetic image sequence, except in this one the $x$-coordinate for the wall is 400 pixels for 20 frames, then 0 for 20 frames and 400 pixels for a further 20 frames. When the wall plane value changes for the first time, error correction is invoked and slowly more correct members are added to the pool of nearest neighbours, but when the wall plane value reverts back to the original value the same process repeats - highlighted in Figure 7.

The FVG method avoids these problems because the multiple associated value distributions can represent different values the features have been mapped to in the sequence so far.

## 5 CONCLUSIONS

We have presented a general update to 3D scene recovery methods which takes advantage of temporal information to increase efficiency. As such, 3 different implementations were provided and applied to an existing 3D scene recovery method. Of which, the simple nearest neighbour methods are affected by the problems of convergence and oscillatory behaviour. The Gaussian model presented copes well with both of these problems, reducing the search space traversal by an order of magnitude and maintaining accuracy of recovered scenes. Now that we have demonstrated the advantages and pitfalls of these methods, we wish to further investigate the benefits of the TSR concept, integrating it with other methods and applying it to more challenging data.

## REFERENCES


Bay, H., Ess, A., Tuytelaars, T., and Gool, L. V. (2008). Surf: Speeded up robust features. *Computer Vision and Image Understanding (CVIU)*, 110(3):346–359.

Chekhlov, D. and Mayol-Cuevas, W. (2008). Appearance based indexing for relocalisation in real-time visual slam. In *19th British Machine Vision Conference*, pages 363–372.

Davison, A. J. (2003). Real-time simulataneous localization and mapping with a single camera. In *Proc. International Conference on Computer Vision*, pages 1403–1411.

Davison, A. J., Reid, I. D., Molton, N. D., and Stasse, O. (2007). Monoslam: Real-time single camera slam. In *IEEE Transactions on Pattern Analysis and Machine Intelligence*, volume 29, pages 1–15.

Fabbri, R. and Kimia, B. (2010). 3d curve sketch: Flexible curve-based stereo reconstruction ad calibration. In *2010 IEEE Conference on Computer Vision and Pattern Recognition*, pages 1538–1545.

Favaro, P., Jin, H., and Soatto, S. (2003). A semi-direct approach to structure from motion. In *The Visual Computer*, volume 19, pages 377–384.

Grinberg, M., Ohr, F., and ad J. Beyerer, D. W. (2010). Feature-based probabilistic data association and tracking. In *The 7th International Workshop on Intelligent Transportation (WIT2010)*, pages 29–34.

Klein, G. and Murray, D. (2007). Parallel tracking and mapping for small ar workspaces. In *Proceedings and the Sixth IEEE and ACM International Symposium on Mixed and Augmented Reailty (ISMAR07)*.

Li, J., Li, ., Chen, Y., Xu, L., and Zhang, Y. (2010). Bundled depth-map merging for multi-view stereo. In *2010 IEEE Conference on Computer Vision and Pattern Recognition*, pages 2769–2776.

Li, P., Farin, D., Gunnewiek, R. K., and de With, P. H. N. (2006). On creating depth maps from monoscopic video using structure frm motion. In *27th Symposium on Information Theory*, pages 508–515.

Warsop, T. E. and Singh, S. (2010). Robust three-dimensional scene recovery from monocular image pairs. In *9th IEEE International Conference on Cybernetic Intelligent Systems 2010 (CIS 2010)*, pages 112–117.

Zhang, G., Dong, Z., Jia, J., Wong, T.-T., and Bao, H. (2010). Efficient non-consecutive feature tracking for structure-from-motion. In *ECCV 2010*, pages 422–435.

Zhang, G., Jia, J., Wong, T.-T., and Bao, H. (2009). Consistent depth maps recovery from a video sequence. In *IEEE Transactions on Pattern Analysis and Machine Intelligence*, volume 21, pages 974–988.